https://doi.org/10.5194/egusphere-2024-3801
Preprint. Discussion started: 7 January 2025
© Author(s) 2025. CC BY 4.0 License.

# Moisture sources and dynamics over southeastern Tibetan Plateau reflected in dual water vapor isotopes

Zhongyin Cai[1*], Rong Li[1], Cheng Wang[1], Qiukai Mao[1], Lide Tian[1]

[1]Institute of International Rivers and Eco-security, Yunnan Key Laboratory of International Rivers and Transboundary Eco-security, Ministry of Education Key Laboratory for Ecosecurity of Southwest China, Yunnan University, Kunming, China

*Corresponding author: Zhongyin Cai (czypil@gmail.com and z.cai@ynu.edu.cn)

**Abstract**

The Tibetan Plateau (TP) serves as a water tower for major rivers in Asia, and mountain valleys in southeastern TP are key channels for moisture entering the TP. Water resources on the TP are experiencing spatially opposite changes due to climate change, and understanding the sources and dynamics of atmospheric moisture is vital. To investigate the role of ocean surface evaporation, continental air mass intrusion, and rain-vapor interaction, we present a three-year daily time series of near-surface water vapor isotope compositions ($\delta^{18}O$ and *d*-excess) from the South-East TP station. We find that apparent negative correlations between *d*-excess and relative humidity over the Indian Ocean mainly reflect their similar seasonality. When analyzed for different seasons, the correlation is insignificant or only explains a marginal fraction of variance. Therefore, caution is required when interpreting the *d*-excess as a conservative tracer of ocean surface evaporation. Instead, local and upstream specific humidity is the

https://doi.org/10.5194/egusphere-2024-3801
Preprint. Discussion started: 7 January 2025
© Author(s) 2025. CC BY 4.0 License.

main factor determining non-monsoon season *d*-excess variability due to the intrusion of cold and dry air from upper levels. During the summer monsoon season, *d*-excess and $\delta^{18}O$ mainly reflect the effect of raindrop evaporation on humidity during transport which decreases lower vapor $\delta^{18}O$ but increases *d*-excess values. These findings provide new insights into the significance of using water isotopes to track moisture sources and dynamics over the TP with seasonally alternating circulation systems. Particularly, the findings for *d*-excess will improve the understanding of different moisture sources and guide the interpretation of *d*-excess derived from other water bodies and ice cores.

## 1 Introduction

The Tibetan Plateau (TP) and its surrounding regions, ~~also termed~~ the Third Pole and the Asian Water Tower, form the highest and largest plateau on Earth ~~that~~ influences climatic and hydrological systems at regional to global scales, such as the ~~formation~~ of the Asian Summer Monsoon (Wu et al., 2022; Yao et al., 2022). In addition, the TP stores the largest amount of frozen water outside of polar regions and sustains freshwater supplies of major river systems in Asia. However, the water balance on the TP has experienced significant changes under the backdrop of global warming (Yao et al., 2022). ~~For instance, the southeastern TP is experiencing a drying trend while wetting in the northern TP (Jiang et al., 2023; Zhang et al., 2023). Atmospheric water vapor is the input of the water storage system and understanding its sources and dynamics is vital for understanding the imbalance of TP's hydrological system.~~

Water stable isotopes are natural tracers of the water cycle (Bowen et al., 2019; Galewsky et al., 2016) and have been intensively studied on the TP in precipitation, surface water, and ice cores (Yao et al., 2013; Thompson et al., 2024; Bershaw, 2018). In general, precipitation isotope ratios ($\delta^{18}O$ and $\delta^{2}H$) over the southern TP have lower values during the summer monsoon season and higher values during ~~the~~ non-monsoon season under the influence

https://doi.org/10.5194/egusphere-2024-3801
Preprint. Discussion started: 7 January 2025
© Author(s) 2025. CC BY 4.0 License.

of the westerlies (He et al., 2015; Tian et al., 2007; Guo et al., 2024; Yang et al., 2017). Recent studies have confirmed that monsoon convection at upstream along moisture transport pathways, rather than local precipitation amount, is the key process that controls summer monsoon season precipitation $\delta^{18}O$ (Cai et al., 2017; He et al., 2015). Different processes have been proposed to elucidate the relationship between precipitation $\delta^{18}O$ and convection where the amount effect (Dansgaard, 1964) is present (Bowen et al., 2019; Galewsky et al., 2016). A relatively classical interpretation is that the continuous rainout associated with stronger convection could cause depleted precipitation following the Rayleigh distillation (Cai and Tian, 2016; Scholl et al., 2009; Vuille et al., 2003). Another interpretation emphasized the role of rain-vapor interaction that partial evaporation of raindrops formed at higher altitudes isotopically depletes lower tropospheric water vapor and then affects subsequent precipitation isotope compositions (Risi et al., 2008a; Kurita et al., 2011; Cai et al., 2018; Lee and Fung, 2008). Observations of vapor isotope compositions could help disentangle the different processes involved in the amount effect, especially the secondary parameter deuterium excess (*d*-excess). The *d*-excess is defined as $\delta^2H$ - $8\delta^{18}O$ by Dansgaard (1964) and mainly reflects the effects of kinetic fractionation. The rainout process mostly involves equilibrium fractionation while raindrop evaporation is associated with kinetic fractionation, and they can therefore have different *d*-excess signatures in water vapor. Isotopic compositions in the vapor phase have only been observed at a few stations on the TP and isotope ratios (δ values) have been the major focus of previous studies (Tian et al., 2020; Dai et al., 2021; Chen et al., 2024; Yu et al., 2016; Yu et al., 2015), less is known about vapor *d*-excess.

It is less certain regarding what caused higher isotope ratios during the non-monsoon season. Following the regional amount effect (Galewsky et al., 2016; Bowen et al., 2019), high $\delta^{18}O$ values could be explained by weakened convection during the non-monsoon season. However, precipitation $\delta^{18}O$ is lower during late- to post-monsoon season in regions extending from the southeastern TP to the head of the Bay of Bengal (BOB), which is not consistent with the weakening of convection (Breitenbach et al., 2010; Cai and Tian, 2020). Shifts of moisture

https://doi.org/10.5194/egusphere-2024-3801
Preprint. Discussion started: 7 January 2025
© Author(s) 2025. CC BY 4.0 License.

transport pathways between convection active and non-active regions have been invoked to explain this abnormal seasonal pattern (Cai and Tian, 2020; Lekshmy et al., 2022). On the other hand, higher precipitation $\delta^{18}O$ accompanied by higher *d*-excess during ~~the~~ non-monsoon season has been interpreted as more intense continental recycling or moisture from the Mediterranean delivered by the westerlies compared with moisture from the Indian Ocean during the summer monsoon (Tian et al., 2007; Yao et al., 2013; An et al., 2017; Breitenbach et al., 2010). In addition, understanding of the atmospheric water cycle for a full seasonal cycle is complicated by the lack of precipitation during the non-monsoon season which can be compensated by monitoring atmospheric water vapor isotopes as it is not limited by precipitation events.

Both theoretical predictions and observations over ocean surface suggested that *d*-excess reflects ocean surface evaporation conditions, such as sea surface temperature (SST) and relative humidity normalized to SST ($RH_{SST}$) (Merlivat and Jouzel, 1979; Bonne et al., 2019; Liu et al., 2014; Craig and Gordon, 1965). Interpretations of *d*-excess over the TP also frequently invoke these relationships with ocean evaporation conditions (Zhao et al., 2012; Shao et al., 2021; Chen et al., 2024; Liu et al., 2024). However, relationships with either $RH_{SST}$ or SST are much weaker than those observed over ocean surface. For instance, Shao et al. (2021) showed significant correlations between an ice core *d*-excess record derived from the central TP and $RH_{SST}$ over the northern BOB and Arabian Sea (AS). However, the correlation coefficient is only -0.44 and the slope between *d*-excess and $RH_{SST}$ is as steep as -0.99‰ $\%^{-1}$. The slope over oceanic regions generally ranges from -0.3‰ $\%^{-1}$ to -0.6‰ $\%^{-1}$ based on in-situ observations (Bonne et al., 2019; Liu et al., 2014; Benetti et al., 2014; Uemura et al., 2008). Many studies have suggested that *d*-excess at terrestrial sites is not a conservative tracer of evaporation conditions at the oceanic source regions (Fiorella et al., 2018; Aemisegger et al., 2014; Welp et al., 2012; Wei and Lee, 2019; Samuels‐Crow et al., 2014). Besides temporal variations, ice core *d*-excess values are generally higher than that observed in precipitation at lower altitudes on the TP (Shao et al., 2021; Tian et al., 2001; Zhao et al., 2012; Joswiak et al., 2013; Zhao et al.,

https://doi.org/10.5194/egusphere-2024-3801
Preprint. Discussion started: 7 January 2025
© Author(s) 2025. CC BY 4.0 License.

2017; Thompson et al., 2000). It is still unclear what caused the abnormally high *d*-excess in these high-altitude ice cores relative to precipitation and river isotope observations at lower altitudes.

Mountain valleys in the southeastern TP are believed to be major moisture transport channels delivering water vapor toward the TP (Araguás-Araguás et al., 1998; Tian et al., 2007; Yao et al., 2013). Therefore, we started a water vapor sampling campaign at the South-East Tibetan Plateau Station for integrated observation and research of alpine environment (SETP) in June 2015 to study the moisture sources and dynamics and their influence on water isotope compositions. Following the previous study (Yao et al., 2013), we define June-September (JJAS) as the summer monsoon season. In contrast, we define November-April (Nov-Apr) as the non-monsoon season and May and October as the transition between the two seasons. We will show distinct seasonal moisture sources and dynamics between the two seasons as reflected in our vapor isotope observations and Lagrangian moisture source diagnostic. Our results suggest that the apparent correlation between SETP vapor *d*-excess and oceanic surface evaporation conditions is mainly a result of their similar seasonality. Alternatively, we suggest the intrusion of dry and cold air by the westerlies from high altitudes contributes to high *d*-excess. In contrast, vapor $\delta^{18}O$ and *d*-excess confirm the significant role of rain-vapor interaction in the amount effect during the summer monsoon season.

## 2 Data and methods

### 2.1 Atmospheric water vapor sampling

~~Atmospheric water~~ vapor samples were collected using a cryogenic trapping method at the SETP station (29°46'N, 94°44'E, 3326 m above sea level, and Fig. S1). The sampling system includes an air pump ~~pumping ambient air into~~ the cold trap, a linked-ball-shaped glass cold trap, and an electric-powered system that creates and maintains a cold environment filled by 95% ethanol as cold as below -80 °C. Ambient air was pumped from an inlet at approximately 8 m above ground level through a Teflon tube to a glass trap immersed in a cold environment with

https://doi.org/10.5194/egusphere-2024-3801
Preprint. Discussion started: 7 January 2025
© Author(s) 2025. CC BY 4.0 License.

a temperature at -70 °C. The airflow rate was adjusted to ~5 L/min to allow 10-20 ml of water samples throughout each sampling operation. During summers, the duration of each sampling operation is 24 hours. During dry winters, however, we increased the sampling duration to 48 hours if a 24-hour sampling period cannot guarantee enough sample amount. The samples were collected at 20:00 Beijing Standard Time (12:00 UTC). The efficiency of extracting water vapor from ambient air was tested by connecting an additional cold trap to the outlet of the initial cold trap, and no visible condensation was noticed in the additional cold trap (Yu et al., 2015). Further comparison against direct measurements of vapor isotope composition by the Picarro L2130-i Cavity Ring Down Spectroscopy (CRDS) at Lhasa, southern TP also confirmed the reliability of this method in sampling atmospheric water vapor over the TP (Tian et al., 2020).

The sampling campaign was started on 25 June 2015 and ended on 14 June 2018. In total, 742 samples were collected, and all the collected samples were kept frozen until transportation to the laboratory for measurements. Samples collected before 28 June 2016 were measured at the Key Laboratory of Tibetan Plateau Earth System, Environment and Resources, Institute of Tibetan Plateau Research, Chinese Academy of Sciences by a Picarro L2130-i analyzer. Samples collected after 28 June 2016 were measured at the Institute of International River and Eco-security, Yunnan University by a Picarro L2140-i analyzer. The isotopic values are calibrated and expressed relative to Vienna Standard Mean Ocean Water 2 (VSMOW2). The precisions of measurements at both laboratories are 0.1‰ for $\delta^{18}O$, 0.4‰ for $\delta^{2}H$, and 1.2‰ for *d*-excess.

**2.2 Meteorological data**

Daily local meteorological data before 2018, including precipitation amount, air temperature, air pressure, and relative humidity, at the SETP station were provided by the station at the National Tibetan Plateau / Third Pole Environment Data Center (Luo, 2018). Specific humidity ($q$) at SETP station is calculated from air temperature, air pressure, and relative humidity at the station.

https://doi.org/10.5194/egusphere-2024-3801
Preprint. Discussion started: 7 January 2025
© Author(s) 2025. CC BY 4.0 License.

To facilitate analyses on larger spatial scales, we obtained meteorological variables (including 2-meter air temperature, 2-meter dew point temperature, and SST, etc.) at 0.25°×0.25° and hourly resolution from the European Centre for Medium-Range Weather Forecasts fifth generation reanalysis (ERA5) (Hersbach et al., 2019). $RH_{SST}$ is estimated from ERA5 2-meter meteorological data and SST using $RH_{SST} = e_{air}/e_{sat}$, where $e_{air}$ is vapor pressure of air and $e_{sat}$ is saturation vapor pressure with respect to SST. We further obtained precipitation data at 0.1°×0.1° and half-hourly resolution from the Integrated Multi-satellitE Retrievals for GPM (V07) (Huffman et al., 2023). In addition, meteorological data at 1°×1° and 3-hourly resolution from the Global Data Assimilation System (GDAS) are used to calculate air mass trajectories (see section 2.4).

**2.3 Theoretical framework for the understanding of isotope compositions and humidity**

Besides complex atmospheric circulation models, the evolution of vapor isotope compositions during different moistening and dehydration processes can be understood by a compilation of atmospheric processes, such as condensation, mixing, and raindrop evaporation, that lead to different pathways of isotopic evolution along atmospheric humidity (Noone, 2012; Worden et al., 2007; Galewsky et al., 2016). The progressive condensation of water vapor and removal as rain droplets or ice is best described by the canonical Rayleigh distillation model (Dansgaard, 1964). In the Rayleigh distillation framework, condensate is removed from the air mass as soon as it forms, and the isotope ratio of remaining vapor is described as $\delta = (1 + \delta_0)(q/q_0)^{\alpha-1} - 1$, where $\delta$ is the isotope composition expressed as per mil deviation from a standard, $q$ is the specific humidity, and $\alpha$ is the fractionation factor. A subscript of 0 refers to the initial condition of the air mass. The falling raindrop may partially evaporate or exchange isotopes with ambient vapor. As raindrops are formed at higher altitudes where water vapor is depleted in heavy isotopes, the partial evaporation of raindrops would preferentially deplete its surrounding water vapor but increase the atmospheric humidity, which leads to $\delta$ values lower than that predicted by the Rayleigh distillation (Risi et al., 2008a; Worden et al., 2007). The evolution of $\delta$ along with $q$ under partial evaporation of

https://doi.org/10.5194/egusphere-2024-3801
Preprint. Discussion started: 7 January 2025
© Author(s) 2025. CC BY 4.0 License.

raindrops can be described in a "super-Rayleigh" trajectory by inflating the effective fractionation factor ($\alpha_e$) as $\alpha_e = (1+\phi)\alpha$, where $\phi$ quantifies the degree to which $\alpha$ deviates from equilibrium. We note that Worden et al. (2007) and Noone (2012) have given different equations to quantify the deviations of $\alpha_e$ from $\alpha$ under different degrees of raindrop evaporation, and the same deviation of $\alpha_e$ from $\alpha$ requires very different degrees of raindrop evaporation. In this study, we follow the formulations by Noone (2012). Finally, the influence of air mass mixing on humidity and isotopic compositions can be modeled through the mass balance perspective. When considering mixing a dry air mass with a moist air mass, for instance, the specific humidity of mixed air mass can be described as $q = f_{dry}q_{dry} + f_{moist}q_{moist}$, where $f$ is the fraction of each air mass with the subscript denoting different air masses and $f_{dry} + f_{moist} = 1$. Isotopic compositions of the mixed air mass can be derived similarly by solving the mass balance equations for the light and heavy isotopes, respectively. The outcome of the mixing process leads to a hyperbolic relationship between $\delta$ and $q$. In other words, $\delta \times q$ and $q$ should have a linear relationship in the mixing process (Fiorella et al., 2018). In a framework of the Keeling plots (Keeling, 1958), the intercept of the regression between $\delta$ and $1/q$ or the slope between $\delta \times q$ and $q$ gives an estimation of the isotope composition of the moist end member.

Assuming a surface temperature of 25 °C and relative humidity of 85%, following the evaporation model by Craig and Gordon (1965) we can derive that $\delta^{18}O$ of ocean surface evaporation is -11.5‰, $\delta^2H$ = -81.4‰, and *d*-excess = 10.6‰. We use this isotopic signature of evaporated water vapor as a wet end member to model the moistening process by mixing with ocean surface evaporation. A hypothetical dry end member from the Rayleigh curve at $q$ = 0.5 g/kg is chosen to represent the dehydrated dry air. The dehydration process by condensation is modeled by choosing a starting point at the mixing line with a relative humidity of 80%. Similarly, the "super-Rayleigh" distillation with partial rain evaporation is started from the same starting point. For the cases of "super-Rayleigh", we simulated the isotopic evolution under two scenarios (Rain_evap_A and Rain_evap_B). Following

https://doi.org/10.5194/egusphere-2024-3801
Preprint. Discussion started: 7 January 2025
© Author(s) 2025. CC BY 4.0 License.

the equations in Noone (2012), Rain_evap_A represents that 2% of rain is evaporated and Rain_evap_B represents an evaporated fraction of 5%. Mixing with evapotranspiration over south Asia and the TP is another way that could modify the atmospheric humidity and vapor isotope compositions over southeastern TP. Accurate quantification of the isotopic composition of land surface evapotranspiration is challenging. Given that the precipitation $\delta^{18}O$ over south Asia is generally between -1.0‰ and -5.0‰ (Bowen and Wilkinson, 2002; Terzer-Wassmuth et al., 2021) and transpiration may account two-thirds of evapotranspiration or more (Cao et al., 2022; Han et al., 2022; Good et al., 2015), we assume the $\delta^{18}O$ of land surface evapotranspiration has a value of -5.0‰ as an upper bound. Similarly, we assume that the *d*-excess of the wet end member of land surface evapotranspiration is 15.0‰.

### 2.4 Air mass trajectory and moisture source diagnostic

Air mass backward trajectories were calculated to investigate the air mass transport and diagnose moisture sources and transport pathways toward SETP using the Hybrid Single-Particle Lagrangian Integrated Trajectory model (HYSPLIT) (Stein et al., 2015). Trajectory calculation is driven by the meteorological data of the GDAS. We released air parcels from 5 locations (the studied site and points displaced 0.2° in each cardinal direction) at 7 different vertical levels at 10, 50, 100, 200, 300, 400, and 500 m above ground level. For each day during the sampling campaign, trajectories were initiated every 3 hours to calculate 10-day backward trajectories. In this setting, 280 trajectories were derived for each single day. Geographical and meteorological variables, including location, pressure, temperature, specific humidity, rainfall amount, boundary layer height, and the terrain height along trajectories, were stored at hourly intervals.

Moisture contribution along air mass trajectories to the humidity at SETP is quantified using the Lagrangian moisture source diagnostic method of Sodemann et al. (2008). The method considers mass balance along the trajectory and assigns increases in specific humidity (forward in time) as moisture uptake, and decreases in specific humidity as moisture lost due to precipitation. The method also proportionally considers the decreased contribution

https://doi.org/10.5194/egusphere-2024-3801
Preprint. Discussion started: 7 January 2025
© Author(s) 2025. CC BY 4.0 License.

of early uptake due to the precipitation en route. We have previously adapted this method to quantify the moisture sources of precipitation in sub-regions of South Asia and East Asia (Cai et al., 2018; Cai and Tian, 2020). The diagnostic results suggest that the unattributed fraction of moisture arriving at SETP is ~5%, and therefore 10-day trajectories are capable of diagnosing most of the moisture sources. Instead of focusing on quantifying the evaporative moisture source from the Earth surface, in this study, we focus on the contribution of the air parcel itself to the humidity at SETP. This variable is readily available from the diagnostic method, and the change of air parcel contributions between time steps within the boundary layer is the moisture uptake from the Earth surface. The moisture contribution by air parcel to humidity at SETP gives a measure of the importance of upstream air masses. Using this variable as the weight, mean upstream geographical and meteorological variables are hence calculated as weighted means. We also applied cluster analysis on the trajectories to visualize the major transport pathways using the K-means clustering method. When calculating the mean trajectory for each cluster and meteorological variables along each mean trajectory, the moisture contribution by air parcel is also considered as the weight to calculate weighted means.

## 3 Results

### 3.1 General characteristics

In general, water vapor $\delta^{18}O$ values are at a lower level during the summer monsoon season and a higher level during the non-monsoon season (Fig. 1a). Mean vapor $\delta^{18}O$ values are -18.4‰ for the non-monsoon season, -23.3‰ for the summer monsoon season, -16.9‰ for May, and -22.8‰ for October. During the onset of the summer monsoon, the vapor $\delta^{18}O$ shows a dramatic decrease to lower values. Without a sharp rebound to values before the summer monsoon, the $\delta^{18}O$ ~~value~~ shows a gradual increase trend from the end of the summer monsoon season ~~toward~~ the highest values during spring and early summer. Although this region is significantly influenced by the

https://doi.org/10.5194/egusphere-2024-3801
Preprint. Discussion started: 7 January 2025
© Author(s) 2025. CC BY 4.0 License.

amount effect, the seasonal trend of vapor $\delta^{18}O$ does not strictly follow the seasonal variation of local precipitation. For instance, local precipitation shows clear cessation after the summer monsoon (Fig. 1e) while $\delta^{18}O$ does not rebound to the level before summer monsoon onset. These seasonal characteristics of vapor $\delta^{18}O$ is consistent with precipitation $\delta^{18}O$ observed in southeastern TP, northeast India, and Bangladesh (Yao et al., 2013; Cai and Tian, 2020; Yang et al., 2017). Overall, water vapor *d*-excess also has lower values during the summer monsoon season and higher values during ~~the~~ non-monsoon season (Fig. 1b). Mean vapor *d*-excess values are 18.3‰ for the non-monsoon season, 11.9‰ for the summer monsoon season, 13.7‰ for May, and 14.9‰ for October. However, the timing of the seasonal transition of vapor *d*-excess is different from that of vapor $\delta^{18}O$. The highest vapor *d*-excess values generally occur during winter months when the air temperature and relative humidity (RH) are the lowest (Fig. 1c and 1d) and the *d*-excess starts to decrease from spring ~~which is~~ earlier than the sharp drop of vapor $\delta^{18}O$ during the onset of the summer monsoon.

https://doi.org/10.5194/egusphere-2024-3801
Preprint. Discussion started: 7 January 2025
© Author(s) 2025. CC BY 4.0 License.

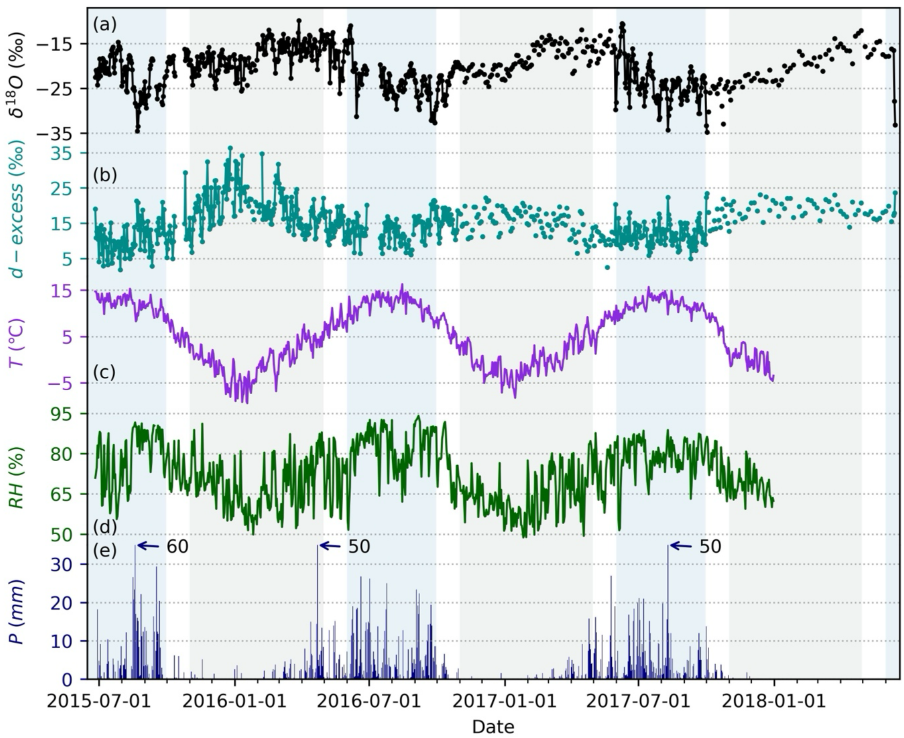


**Figure 1. The general temporal variability of observed water vapor isotope compositions and daily local meteorological variables from 2015-2018: (a) δ$^{18}$O, (b) *d*-excess, (c) air temperature, (d) relative humidity (RH), and (e) precipitation amount. The light blue shading highlights the summer monsoon season and the light steel blue shading highlights the non-monsoon season.**

The linear relationship between paired δ$^{18}$O and δ$^{2}$H ~~data points~~ and ~~their locations~~ relative to the global meteoric water line (GMWL, δ$^{2}$H = 8δ$^{18}$O + 10) (Craig, 1961) ~~generally~~ provide additional insights into isotopic fractionation (Putman et al., 2019). The local meteoric water line (LMWL) estimated from all vapor δ$^{2}$H and δ$^{18}$O data points is δ$^{2}$H = 7.96δ$^{18}$O + 14.04 ($R^2$ = 0.98) which plots above but approximately parallel with the GMWL. This relatively higher intercept of vapor LMWL reflects the continental location of the site and further kinetic fractionation after ocean surface evaporation. The δ$^{2}$H-δ$^{18}$O relationship also varied seasonally. The vapor LMWL

https://doi.org/10.5194/egusphere-2024-3801
Preprint. Discussion started: 7 January 2025
© Author(s) 2025. CC BY 4.0 License.

for non-monsoon season is $\delta^2H = 7.58\delta^{18}O + 10.61$ ($R^2 = 0.96$) and for summer monsoon season is $\delta^2H = 7.53\delta^{18}O + 0.91$ ($R^2 = 0.99$). Non-monsoon season vapor isotope compositions mainly plot above the GMWL and even above the overall vapor LMWL. While the majority of monsoon season isotope data plot below the overall vapor LMWL, those data points that have the lowest δ values plot above the overall vapor LMWL indicating further kinetic fractionation such as rain evaporation. Vapor isotope compositions for May are more similar to those during the non-monsoon season but plot closer to the GMWL and LMWL, while data for October show a more similar behavior with the monsoon season observations.

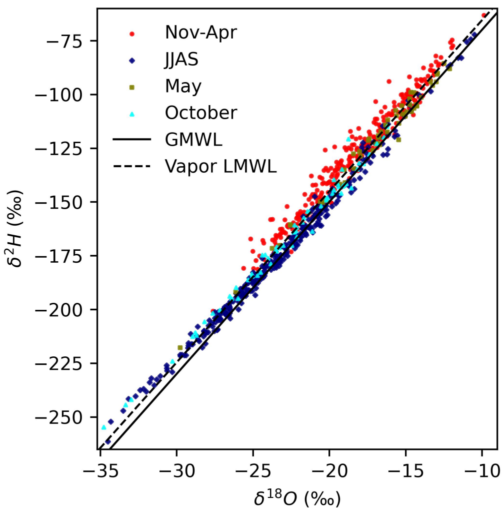


**Figure 2. Relationship between vapor $\delta^2$H and $\delta^{18}$O. Data during the non-monsoon season (Nov-Apr), the summer monsoon season (JJAS), May, and October are shown as red dots, navy diamonds, olive squares, and cyan trangles, respectively. The solid line indicates the global meteoric water line (GMWL). The dashed line indicates the local meteoric water line (LMWL) estimated from all vapor $\delta^2$H and $\delta^{18}$O data points.**

The relationships between vapor $\delta^{18}O$ and specific humidity ($q$) further indicate seasonally contrasting moisture dynamics (Fig. 3a). Note that only data before 2018 are shown as local meteorological data are unavailable in 2018. In addition, the sampling frequency during 2018 was reduced (Fig. 1) due to logistic issues. Therefore,

https://doi.org/10.5194/egusphere-2024-3801
Preprint. Discussion started: 7 January 2025
© Author(s) 2025. CC BY 4.0 License.

when analyzing relationships between vapor isotope compositions ($\delta^{18}$O and *d*-excess) and meteorological variables (both locally and regionally) we only focused on data before 2018. For months during the non-monsoon season, the majority of data points fall above the Rayleigh distillation line but below the mixing line ~~of~~ an upper bound of hypothetical evapotranspiration over South Asia, ~~especially for the winter months~~. In contrast, data for the summer monsoon season months predominately fall below the Rayleigh distillation line and are constrained by "super-Rayleigh" lines with different degrees of rain evaporation. The relationships between $\delta \times q$ and $q$ further indicate seasonal contrast moisture source signatures (Fig. S3). Distribution of non-monsoon season $\delta \times q$ and $q$ suggests the mixing between a dry end member ~~that has almost totally dehydrated through condensation~~ and a moist end member ~~of surface evaporation or moisture that has been partially dehydrated through Rayleigh distillation~~ (Fig. S3). A simple estimation through the linear regression between $\delta \times q$ and $q$ suggests $\delta^{18}$O of the moist end member for the non-monsoon season is -13.9‰ ± 0.6‰. The amount weighted annual mean precipitation $\delta^{18}$O at ~~this~~ site was about -14.5‰ (Yao et al., 2013). However, the overall estimation for the summer monsoon season suggests $\delta^{18}$O of the moist end member is -30.9‰ ± 1.8‰ which is much lower than the estimation for the non-monsoon season. This exceptionally low value requires an additonal moisture source of rain evaporation that is much depleted in heavy isotopes than surface evapotranspiration ~~and is~~ consistent with the distribution of $\delta^{18}$O-*q* below the Rayleigh distillation line (Fig. 3a).

The relationships between vapor *d*-excess and *q* also ~~suggest~~ seasonal contrasts in moisture dynamics (Fig. 3b). During non-monsoon season months, vapor *d*-excess shows a negative correlation with *q*, and the highest *d*-excess values are generally associated with the driest and coldest air (Figs. 1 and 3b). However, vapor *d*-excess does not show a clear relationship with *q* and shows a substantial variability (~20‰ in range) at a given *q* during the summer monsoon season. These relationships suggest that vapor *d*-excess is less predictable ~~by *q* than~~ $\delta^{18}$O, except ~~for~~ low humidity levels.

https://doi.org/10.5194/egusphere-2024-3801
Preprint. Discussion started: 7 January 2025
© Author(s) 2025. CC BY 4.0 License.

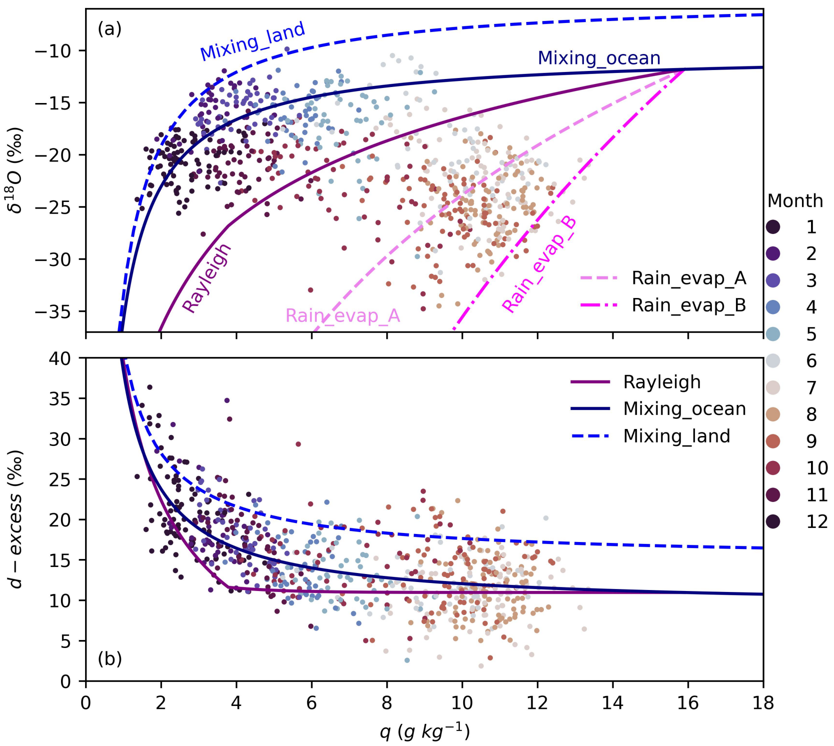


**Figure 3. Relationships between vapor isotope compositions and specific humidity (*q*) from 2015-2017. (a) scatter plot of $\delta^{18}O$ against specific humidity (*q*). (b) scatter plot of *d*-excess against *q*. The months for the data points are color-coded. The reference lines are the same as those in Fig. S2, and interpretations of these reference lines are referred to Fig. S2 and section 2.3.**

## 3.2 Moisture sources and transport pathways for different seasons

To understand drivers of the seasonal contrasting moisture dynamics ~~reflected in vapor isotope compositions~~, we first analyzed the moisture sources and transport pathways during different seasons (Fig. 4). Note again that we focus on the contribution by historical (last 10 days) air mass to humidity at SETP instead of moisture uptake from the Earth surface. During the non-monsoon season, moisture is mainly transported by two branches with one from the west of SETP by the westerlies (clusters Nov-Apr2 and Nov-Apr3) and the other from the south of SETP such

https://doi.org/10.5194/egusphere-2024-3801
Preprint. Discussion started: 7 January 2025
© Author(s) 2025. CC BY 4.0 License.

as the BOB (cluster Nov-Apr1). Quantitatively, the fraction of moisture from the south pathway and the sum of the two west branches is comparable (52.4% vs. 47.7%). We note that if moisture contributions by air parcels are not considered, trajectories for all three clusters are from the west of SETP and they only reflect the transport of air masses (Fig. S4). These differences between pure air mass trajectories and considering moisture contribution by air masses call for caution when interpreting air mass trajectories. During the summer monsoon season, moisture is predominantly transported from the south of SETP by the summer monsoon. The moisture sources and transport pathways for May show some similarities with the ~~results~~ for the non-monsoon season. Compared with the second transport pathway during the non-monsoon (cluster Nov-Apr2), the second transport pathway during May (cluster May2) shows an overall southward shift toward the AS. Although the air mass transport pattern during October is also similar to that during the non-monsoon, the moisture sources and transport pathways for October show similarities with the results for the summer monsoon season with a slight eastward shift (Figs. 4d and S4d).

Another emerging feature of moisture source distributions is that humidity at SETP is predominantly contributed by air masses over proximal terrestrial regions, especially those ~~regions~~ in its south (Fig. 4). In contrast, air masses over oceanic regions make a much smaller contribution to humidity at SETP. For instance, the 1% contour of moisture contribution by air parcels over each 1°×1° grid box does not reach oceanic regions during all four seasons. Therefore, moisture uptake of surface evaporation from oceanic regions, such as from the BOB and AS, is also very limited as most of the moisture in air masses over these oceanic regions is lost by precipitation and replenished by evapotranspiration during the transport toward SETP. This result questions whether vapor isotopic compositions at SETP still preserve the meteorological information at the ocean surface.

https://doi.org/10.5194/egusphere-2024-3801
Preprint. Discussion started: 7 January 2025
© Author(s) 2025. CC BY 4.0 License.

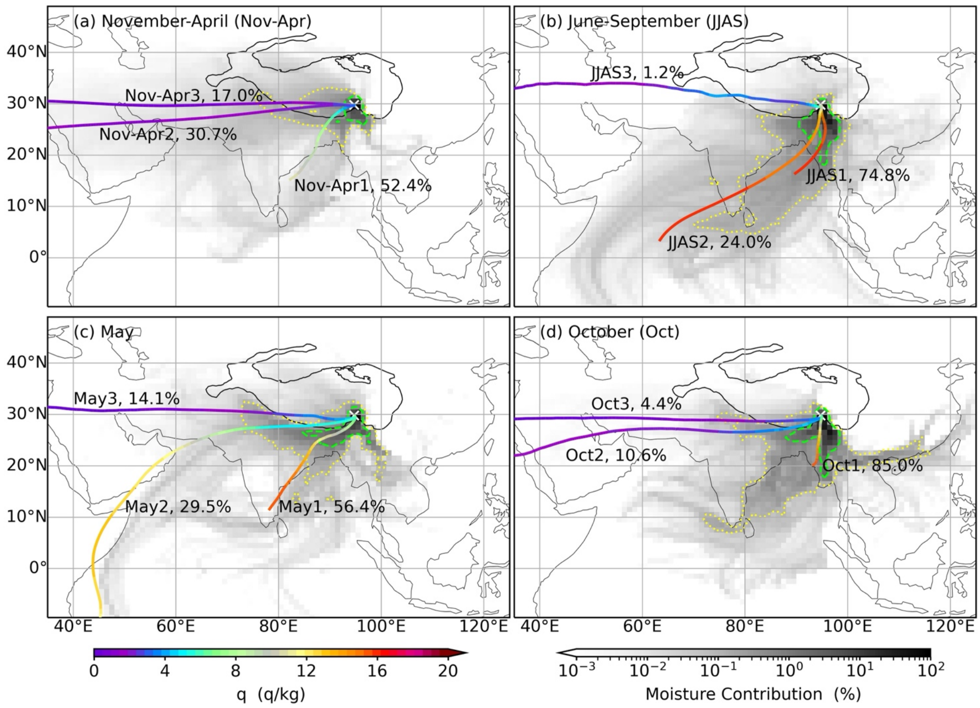


**Figure 4. Moisture sources and transport pathways during different seasons from 2015-2017. (a) spatial distribution of relative contribution of moisture by all air parcels overall each 1°×1° box (shading) to humidity at the SETP station and specific humidity (*q*) along mean trajectories (weighted by the moisture contribution of air parcels) for the non-monsoon season of November-April (Nov-Apr). (b-d) are the same as (a), but for the monsoon season of June-September (JJAS, b), May (c), and October (d), respectivley. The dotted yellow and dashed green contours indicate the moisture contribution at 0.1% and 1%, respectively. The yellow crosses indicate the location of the SETP station. The black solid lines denote the Tibetan Plateau with altitude contour at 3000 m.**

https://doi.org/10.5194/egusphere-2024-3801
Preprint. Discussion started: 7 January 2025
© Author(s) 2025. CC BY 4.0 License.

## 4 Discussion

### 4.1 Role of ocean surface evaporation conditions

Relationships between vapor *d*-excess and ocean surface evaporation conditions ~~of~~ $RH_{SST}$ and SST are first tested using all the data from 2015-2017 (Fig. 5a and Fig. S5a). Results indeed show negative correlations between vapor *d*-excess and $RH_{SST}$ over northern Indian Ocean, especially the northern part of AS and BOB (Fig. 5a). Quantitively, slopes of the regression between *d*-excess and $RH_{SST}$ over the northern Indian Ocean range from higher than -0.1‰ %$^{-1}$ to values below -0.6‰ %$^{-1}$. The regression slopes over the northern BOB (10-22°N and 80-99°E) and the eastern AS (7-20°N and 65-78°E; Fig. 5a) fall within the range reported in previous studies (Uemura et al., 2008; Benetti et al., 2014; Liu et al., 2014; Bonne et al., 2019). Vapor *d*-excess and regional average $RH_{SST}$ yields an overall slope of -0.49‰ %$^{-1}$ ($r = -0.52$ and $p < 0.01$) for the eastern AS (Fig. S6) and -0.52‰ %$^{-1}$ ($r = -0.55$ and $p < 0.01$) for the northern BOB (Fig. S7). However, the distribution of data in the *d*-excess and $RH_{SST}$ space suggests a clustering of data that observations during summer months are mainly located in the lower right with high $RH_{SST}$ and low *d*-excess, but in the upper left part of the space for winter months. During each season, there is substantial variability in vapor *d*-excess for a given $RH_{SST}$. These results suggest that the apparent negative correlation between *d*-excess and $RH_{SST}$ may mainly arise from their opposite seasonality. Similarly, apparent negative correlations between vapor *d*-excess and SST also emerge over the northern Indian Ocean (Fig. S5a). However, both theoretical prediction (Merlivat and Jouzel, 1979) and in-situ observations above the ocean surface (Bonne et al., 2019; Liu et al., 2014) suggest a positive correlation between vapor *d*-excess and SST. Therefore, we argue that the overall correlations between SETP vapor *d*-excess and surface evaporation conditions over the northern Indian Ocean are mainly a result of their seasonality ~~and do not hold realistic causal relation~~ships.

We further examined the relationship between vapor *d*-excess and $RH_{SST}$ for the summer monsoon and non-monsoon seasons, respectively. The negative correlation between vapor *d*-excess and $RH_{SST}$ almost totally

https://doi.org/10.5194/egusphere-2024-3801
Preprint. Discussion started: 7 January 2025
© Author(s) 2025. CC BY 4.0 License.

diminishes, especially during the summer monsoon season when absolute values of correlation coefficients drop to below 0.3 (Fig. 5b). Stronger correlations during the non-monsoon season (Fig. 5c) could be due to the overall intraseasonal variation that *d*-excess is the highest during winter and lower at the beginning and ending stages (Fig. 1b) which could be accompanied with an opposite $RH_{SST}$ trend. Even so, the correlations during the non-monsoon still only explain a marginal fraction of variance in *d*-excess (10%-16% at maximum over the northern BOB). Similarly, correlations with SST over the northern Indian Ocean also become trivial when separately considering the summer monsoon or non-monsoon season (Fig. S5). In summary, vapor *d*-excess at SETP is less likely a conservative tracer of surface evaporation conditions (neither $RH_{SST}$ nor SST) over the northern Indian Ocean. Therefore, it should be cautious when interpreting *d*-excess in meteoric water or paleo archives from the TP as a proxy of evaporation conditions over the Indian Ocean.

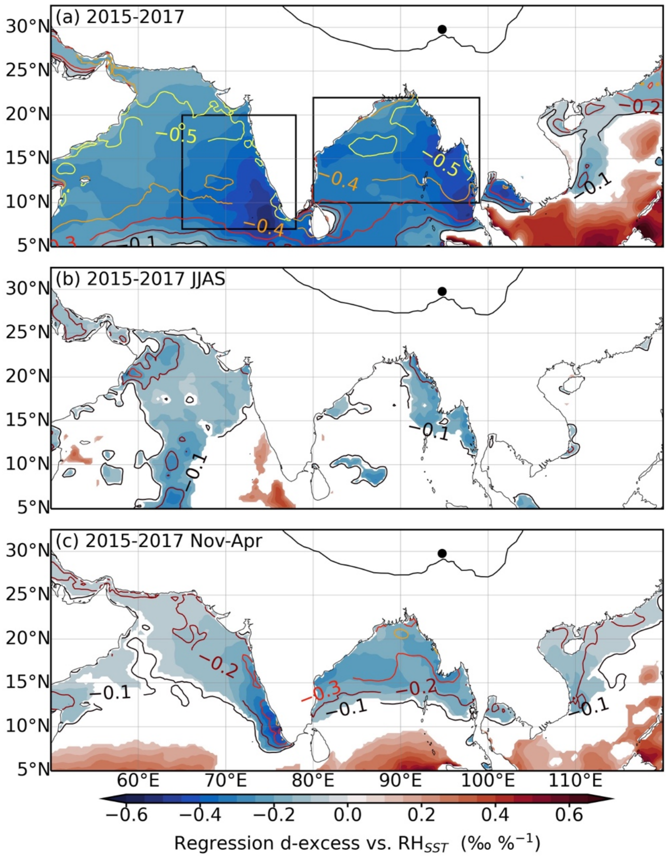


**Figure 5. Relationships between water vapor *d*-excess and relative humidity scaled to sea surface temperature (RH$_{SST}$). (a) regression of vapor *d*-excess against RH$_{SST}$ (shading and only values significant at the 95% significance level are shown) and correlation coefficients between them (contours at an interval of 0.1 and only negative correlations are shown) for all the data from 2015-2017. (b) and (c) are the same as (a) but only for the data within the summer monsoon season (JJAS) or the non-monsoon season (Nov-Apr), respectively. The black dots indicate the location of the SETP station. The black solid lines denote the Tibetan Plateau with altitude contour at 3000 m.**

https://doi.org/10.5194/egusphere-2024-3801
Preprint. Discussion started: 7 January 2025
© Author(s) 2025. CC BY 4.0 License.

### 4.2 Role of dry and cold air intrusion during the non-monsoon season

Both theoretical predictions by the Rayleigh model and observations during the non-monsoon season suggest an increasing trend of vapor *d*-excess when *q* goes to extremely low values (Fig. 2). In addition, results for both air mass transport and moisture transport show the dominant role of the westerlies (Figs. S4a and 4a). Therefore, we hypothesize that the mixing of cold and dry air transported by the westerlies from higher altitudes with surface vapor controls vapor isotope compositions during the non-monsoon season. Surface vapor influenced by recycled moisture from terrestrial evapotranspiration would further elevate vapor *d*-excess at a given *q* (Fig. 3b). We first did a composite analysis on moisture sources and transport pathways for the highest (higher than 30‰ and n = 10) and lowest *d*-excess observations (lower than 10‰ and n = 8) during the non-monsoon season (Fig. 6). For high vapor *d*-excess values, moisture is predominantly transported by westerlies from the west of SETP, such as over the TP and northwestern India. In addition, air masses along backward trajectories are characterized by extremely low *q* i.e. as low as below 2 g $kg^{-1}$ along the mean trajectories (weighted by the moisture contribution) over the TP (Fig. 6a). For low *d*-excess cases, a substantial amount of moisture transport pathways (account for 39.2% by the L1 cluster, Fig. 6b) shift toward more humid areas of northeast India, Bangladesh, and the BOB. This contrasting moisture transport pattern between high and low *d*-excess cases agrees with our hypothesis that the high *d*-excess is associated with dry and cold air transported by the westerlies.

https://doi.org/10.5194/egusphere-2024-3801
Preprint. Discussion started: 7 January 2025
© Author(s) 2025. CC BY 4.0 License.

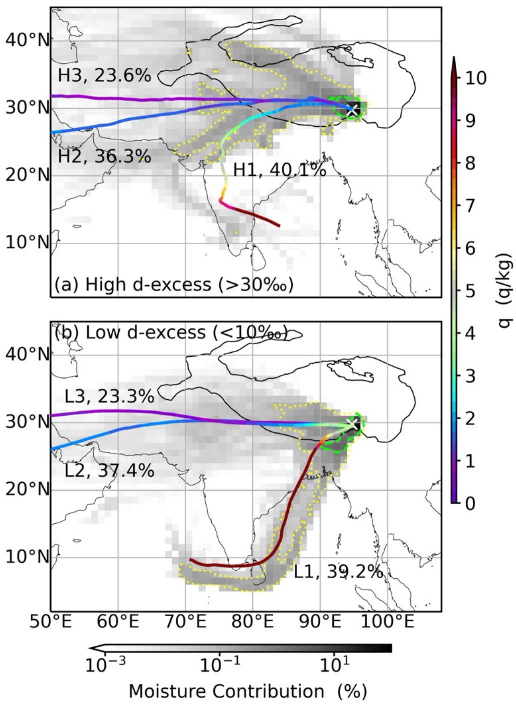


**Figure 6. Composite of moisture sources and transport pathways for high and low *d*-excess days during the non-monsoon season of November-April. (a) spatial distribution of relative contribution of moisture by all air parcels overall each 1°×1° box (shading) to humidity at the SETP station and specific humidity (*q*) along mean trajectories (weighted by the moisture contribution of air parcels) for *d*-excess values higher than 30‰ during the non-monsoon season (n = 10). (b) is the same as (a) but for *d*-excess lower than 10‰ (n = 8). The yellow crosses indicate the location of the SETP station. The black solid lines denote the Tibetan Plateau with altitude contour at 3000 m.**

~~The relationship between vapor *d*-excess and~~ the intrusion of cold and dry air is further tested by relationships among vapor *d*-excess, local *q*, upstream *q*, upstream air temperature, and upstream air altitude (Fig. 7). Upstream variables are mean values along the 10-day backward trajectory weighted by the moisture contribution of the air parcel at each time step (section 2.4). The non-monsoon season vapor *d*-excess shows robust negative correlations

https://doi.org/10.5194/egusphere-2024-3801
Preprint. Discussion started: 7 January 2025
© Author(s) 2025. CC BY 4.0 License.

with $q$ both at the local scale as well as at upstream (r = -0.65 and -0.67, respectively, and p < 0.01 for both). At the same time, low $q$ is associated with air masses with low temperature and from high altitudes (Figs. 7c and 7d). This effect could also have an impact on vapor $\delta^{18}O$. $\delta^{18}O$ during the high *d*-excess cases is lower than $\delta^{18}O$ during the low *d*-excess cases (at a significance level of 95.3%), and the overall correlation coefficient between $\delta^{18}O$ and *d*-excess during the non-monsoon season is -0.29 (p < 0.01). Correlations between $\delta^{18}O$ and local $q$ (r = 0.42 and p < 0.01) or upstream $q$ (r = 0.38 and $p < 0.01$) are weaker than the correlations between *d*-excess and $q$. The relationship between non-monsoon season $\delta^{18}O$ and humidity is mainly expressed as the relationship between $\delta \times q$ and $q$ (r = 0.82 for local $q$ and r = 0.90 for upstream $q$).

We further analyzed the spatial distribution of correlations between ~~SETP~~ vapor isotope compositions ($\delta^{18}O$ and *d*-excess) and 2-meter air temperature as well as humidity measured by 2-meter dew point temperature during the non-monsoon season (Fig. 8). Results show significant negative correlations between *d*-excess and dew point temperature at the regional scale over southeastern TP, northeast India, and northern Bangladesh (Fig. 8a). Correlations with air temperature are generally similar with correlations between *d*-excess and dew point temperature but the most significant correlations are in a smaller region (Fig. 8b). In contrast, correlations between $\delta^{18}O$ and dew point temperature is not as strong as that for *d*-excess (Fig. 8c). Instead, $\delta^{18}O$ shows stronger positive correlations with air temperature over the India subcontinent and the northwestern part of southeast Asia (Fig. 8d).

Extremely high *d*-excess values at very low $q$ levels are predicted in Fig. 3b, and previous study has shown that as $q$ approaches zero, vapor *d*-excess can approach 7000‰ following the Rayleigh distillation trajectory (Bony et al., 2008) caused by the definition of the *d*-excess (Dütsch et al., 2017). High vapor *d*-excess values have also been observed in low humidity conditions such as in the polar regions (Bonne et al., 2014; Steen-Larsen et al., 2017) or at high altitudes (Samuels‐Crow et al., 2014; Webster and Heymsfield, 2003; Sayres et al., 2010; Sodemann et al., 2017). Therefore, we infer that the increasing trend of vapor *d*-excess along with decreasing local $q$, upstream

https://doi.org/10.5194/egusphere-2024-3801
Preprint. Discussion started: 7 January 2025
© Author(s) 2025. CC BY 4.0 License.

*q,* and regional dew point temperature is a result of intensified mixing with dry and cold subsiding air transported by the westerlies from high altitudes. Relationships between upstream *q* and upstream air temperature as well as altitude support this inference that low humidity condition is associated with subsiding dry and cold air from high altitudes (Figs. 7c and 7d). Therefore, vapor *d*-excess during the non-monsoon not only provides information on the specific humidity but also indicates the source of humidity.

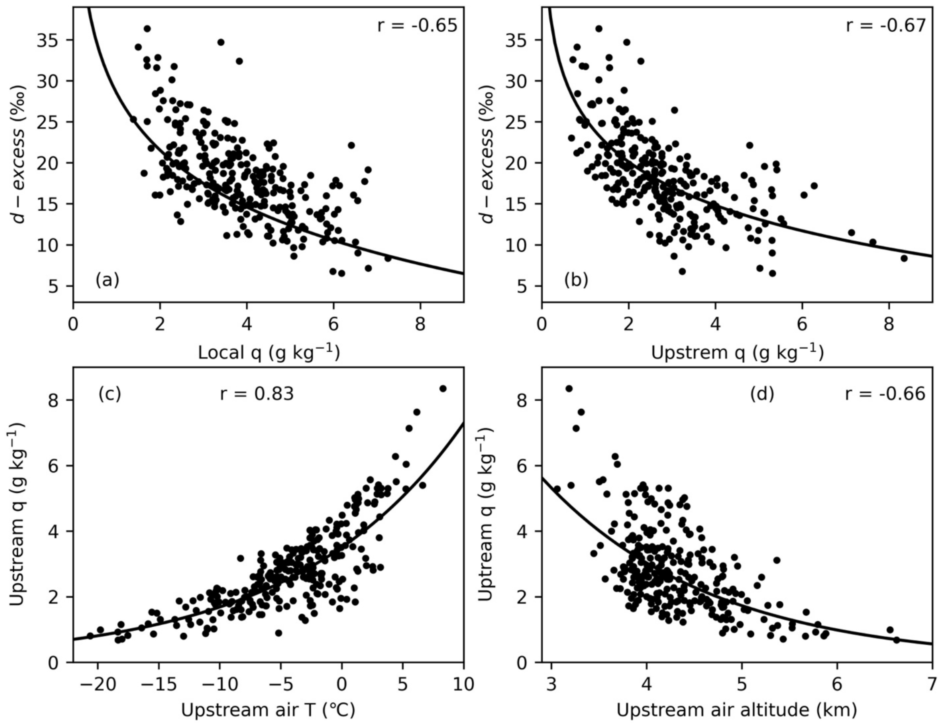


**Figure 7. Relationships among water vapor *d*-excess, local specific humidity (*q*), upstream *q*, upstream air temperature (T), and upstream air altitude during the non-monsoon season of November-April. (a) scatter plot of *d*-excess against local *q*. (b) scatter plot of *d*-excess against upstream weighted-mean *q*. (c) scatter plot of upstream *q* against upstream air T. (d) scatter plot of upstream *q* against upstream air altitude. All the upstream variables are mean values along backward trajectories weighted by the moisture contribution of air parcels. The solid curves indicate the log regression between the respective variables with the correlation**

https://doi.org/10.5194/egusphere-2024-3801
Preprint. Discussion started: 7 January 2025
© Author(s) 2025. CC BY 4.0 License.

**coefficients indicated by the numbers.**

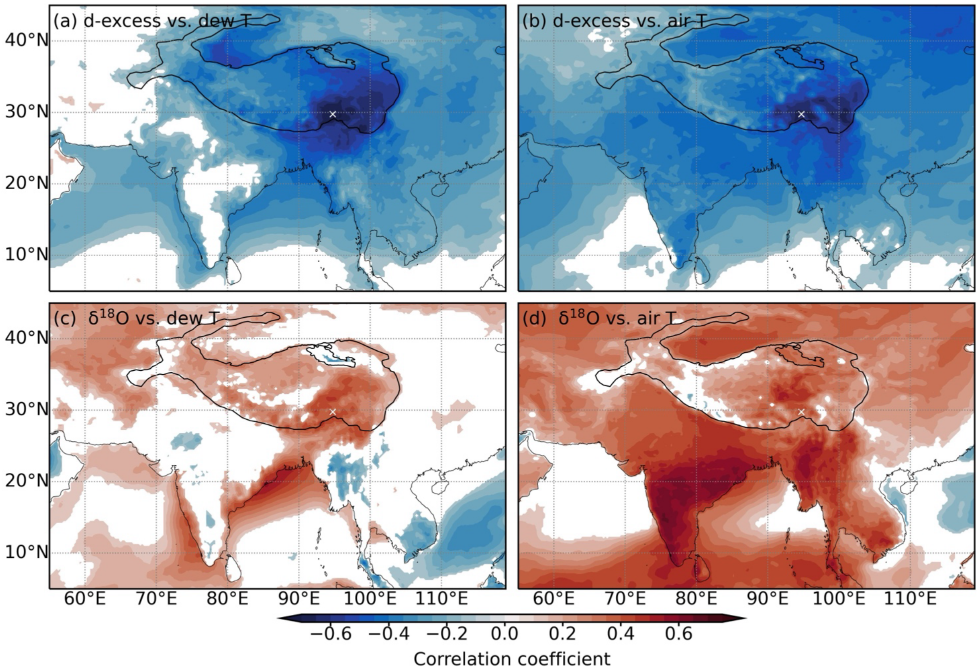


**Figure 8. Spatial distribution of correlation coefficients among water vapor isotope compositions, dew point temperature, and air temperature during the non-monsoon season of November-April. (a) spatial distribution of correlation coefficients between SETP vapor *d*-excess and 2-meter dew point temperature. (b) the same as (a) but with 2-meter air temperature. (c) the same as (a) but between $\delta^{18}O$ and 2-meter dew point temperature. (d) the same as (c) but with 2-meter air temperature. Only values significant at the 95% significance level are shown. The white crosses indicate the location of the SETP station. The black solid lines denote the Tibetan Plateau with altitude contour at 3000 m.**

### 4.3 Role of rain-vapor interaction during the summer monsoon season

Different from the significant dependence of vapor *d*-excess on specific humidity during the non-monsoon season, vapor *d*-excess is not correlated with specific humidity (r = 0.04 and p = 0.51) during the summer monsoon

https://doi.org/10.5194/egusphere-2024-3801
Preprint. Discussion started: 7 January 2025
© Author(s) 2025. CC BY 4.0 License.

season. The behavior of $\delta^{18}O$ is also distinct during the two seasons (Fig. 3). Distribution of summer monsoon season observations in the $\delta^{18}O$-$q$ space suggests that the vapor has undergone a certain degree of rain-vapor interaction by rain evaporation (Fig. 3a). On the other hand, partial rain evaporation in an unsaturated atmospheric environment is associated with kinetic fractionation which decreases the *d*-excess values of the raindrop but increases the *d*-excess of surrounding vapor (Risi et al., 2008b). This effect of rain-vapor interaction on vapor isotope compositions has been suggested as a major process responsible for the amount effect in the tropics (Risi et al., 2008a; Kurita et al., 2011; Bowen et al., 2019; Galewsky et al., 2016). Therefore, we hypothesize that vapor isotope compositions during the summer monsoon season at SETP are controlled by the degree of rain-vapor interaction. The first evidence supporting this hypothesis is that vapor $\delta^{18}O$ is significantly correlated with *d*-excess during the summer monsoon season ($r = -0.55$ and $p < 0.01$, Fig. 9a). In addition, there is a trend that vapor $\delta^{18}O$ and *d*-excess are less correlated when $\delta^{18}O$ is high and the opposite for low $\delta^{18}O$ levels (Figs. 9a and S8). If there is no rain, rain-vapor interaction is not possible. Therefore, we flitted data during days when the daily precipitation amount is not less than 2 mm as rainy days and days with precipitation less than 2 mm as no rain occurs locally (non-rainy days). Vapor $\delta^{18}O$ during rainy days is significantly higher than during non-rainy days and the opposite trend applies for *d*-excess ($p < 0.01$ for both $\delta^{18}O$ and *d*-excess) (Figs. 9b and 9c). The correlation between vapor $\delta^{18}O$ and *d*-excess during rainy days becomes stronger ($r = -0.69$ and $p < 0.01$). However, vapor $\delta^{18}O$ is still negatively correlated with *d*-excess during non-rainy days ($r = -0.40$ and $p < 0.01$). Even if a stricter threshold of 0 mm for daily precipitation amount is used for flittering non-rainy days, there is still a significant negative correlation between vapor $\delta^{18}O$ and *d*-excess ($r = -0.37$ and $p < 0.01$). In addition, correlations with local precipitation amount are weak both for $\delta^{18}O$ ($r = -0.31$ and $p < 0.01$) and *d*-excess ($r = 0.26$ and $p < 0.01$). Therefore, we further infer that the effect of rain-vapor interaction is not only from the local scale but also inherits the history of rain-vapor interaction before vapor has been transported to SETP.

https://doi.org/10.5194/egusphere-2024-3801
Preprint. Discussion started: 7 January 2025
© Author(s) 2025. CC BY 4.0 License.

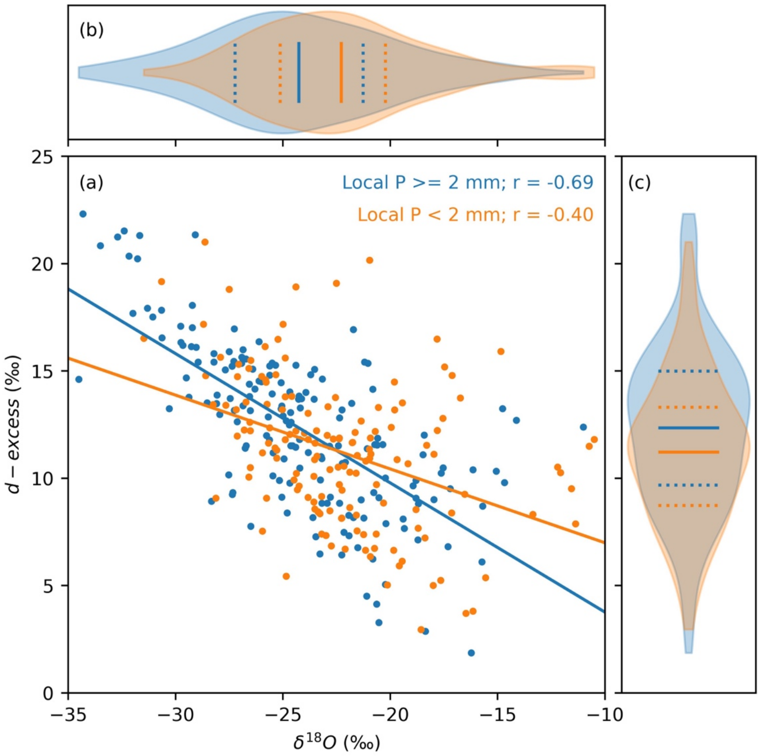


**Figure 9. Relationships between SETP vapor *d*-excess and $\delta^{18}O$ during the summer monsoon season. (a) scatter plot of *d*-excess against $\delta^{18}O$ and linear regression lines between them. (b) distribution of $\delta^{18}O$ values with the dashed lines indicate values at the lower and upper quartiles and the solid lines indicate the mean values. (c) is the same as (b) but for *d*-excess. Orange colors indicate data observed during daily precipitation amount less than 2 mm and blue colors indicate data observed during days with precipitation amount not less than 2 mm.**

If there is a larger amount of rainfall, the effect of rain-vapor interaction on atmospheric humidity would be stronger. Therefore, we use total precipitation amount ($P_{acc}$) as a measure of rain-vapor interaction. To account for the history during moisture transport, the total precipitation amount during several days before sampling is considered. We have tested the relationships between vapor isotope compositions ($\delta^{18}O$ and *d*-excess) and $P_{acc}$ over

https://doi.org/10.5194/egusphere-2024-3801
Preprint. Discussion started: 7 January 2025
© Author(s) 2025. CC BY 4.0 License.

1-10 days prior to sampling (Figs. S9 and S10). Vapor *d*-excess reaches an optimal correlation with $P_{acc}$ when the total precipitation amount during 3 days before sampling ($P_{acc\_3d}$) is considered. Vapor $\delta^{18}O$ shows a slightly longer memory and reaches an optimal correlation with $P_{acc}$ when the total precipitation amount during 5-6 days before sampling is considered. Fig. 10 shows the spatial distribution of correlations between vapor isotope compositions ($\delta^{18}O$ and *d*-excess) and $P_{acc\_3d}$. Vapor *d*-excess shows significant positive correlations with $P_{acc\_3d}$ in the region surrounding SETP with a spatial scale of ~5°×5° and the positive correlation extends southwestward to the foothill of the Himalayas (Fig. 10a). In contrast, vapor $\delta^{18}O$ shows significant negative correlations with $P_{acc\_3d}$ in similar regions (Fig. 10b). For non-rainy days, vapor $\delta^{18}O$ and *d*-excess still show significant correlations with $P_{acc\_3d}$ at regional scale, albeit with weaker correlation levels and smaller spatial extent (Fig. S11). These significant correlations among vapor $\delta^{18}O$, *d*-excess, and $P_{acc\_3d}$ provide further evidence for understanding processes that are responsible for the amount effect. The negative correlation between $\delta^{18}O$ and $P_{acc\_3d}$ has also been observed in precipitation and can be interpreted in terms of either continuous rainout (Cai and Tian, 2016; Scholl et al., 2009; Vuille et al., 2003) or the effect of rain-vapor interaction (Lawrence et al., 2004; Risi et al., 2008a; Kurita et al., 2011; Worden et al., 2007). Although continuous rainout with increased rainfall amount can explain the decreasing trend of $\delta^{18}O$ by the Rayleigh distillation model, *d*-excess stays at a relatively stable level when specific humidity is not very low (above ~4 g $kg^{-1}$ in Fig. 3b for example). Therefore, the positive correlation between vapor *d*-excess and $P_{acc\_3d}$ provides an additional constraint that the amount effect is not simply a result of rainout but ~~rain-vapor interaction plays an important role in altering lower tropospheric isotope compositions.~~

https://doi.org/10.5194/egusphere-2024-3801
Preprint. Discussion started: 7 January 2025
© Author(s) 2025. CC BY 4.0 License.

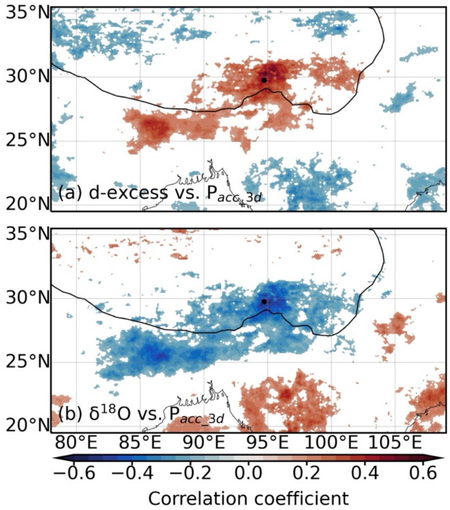


**Figure 10. Relationships between vapor isotope compositions for rainy days (local daily precipitation amount not less than 2 mm) and total precipitation amount at the regional scale during the summer monsoon season. (a) spatial distribution of correlation coefficients between vapor *d*-excess and total precipitation amount during 3 days prior sampling ($P_{acc\_3d}$). (b) is the same as (a) but for $\delta^{18}$O. Only values significant at the 95% significance level are shown. The black dots indicate the location of the SETP station. The black solid lines denote the Tibetan Plateau with altitude contour at 3000 m.**

### 4.4 An alternative interpretation for the high *d*-excess in high-altitude TP ice cores

Interpretations of *d*-excess in meteoric water and ice cores on the TP are complicated by evaporation conditions over the northern Indian Ocean ($RH_{SST}$ and SST) and continental recycling (Shao et al., 2021; Zhao et al., 2012; Joswiak et al., 2013; Pang et al., 2012; An et al., 2017). Attempts have been made to establish a relationship between vapor *d*-excess and $RH_{STT}$ (Chen et al., 2024; Liu et al., 2024) as well as between ice core *d*-excess and $RH_{STT}$ (Shao et al., 2021) or SST (Zhao et al., 2012). Based on relationships between vapor *d*-excess and surface evaporation conditions discussed above, however, the apparent relationships are mainly a result of similarities in the seasonality

https://doi.org/10.5194/egusphere-2024-3801
Preprint. Discussion started: 7 January 2025
© Author(s) 2025. CC BY 4.0 License.

of these variables. Furthermore, the direct contribution of water vapor contained in air masses over oceanic regions to humidity at SETP is very limited (Fig. 4), which implies that the contribution to humidity over the TP is further decreased than at SETP as it is at the forefront of moisture transport toward TP (Fig. S1). The dominant terrestrial origin indicates that the moisture has undergone a certain degree of continental recycling. Mixing with terrestrial sources is also reflected in the relationship between isotope compositions and $q$ (Fig. 3). The degree of continental recycling also alters vapor isotope compositions that transpiration introduces isotopically enriched moisture and evaporation introduces moisture with high $d$-excess. Seasonally changing isotope signatures in precipitation and ice cores as well as variations at longer timescales have been interpreted as moisture source shift between recycled moisture over terrestrial regions and oceanic moisture sources or their relative contributions (An et al., 2017; Yang and Yao, 2020). A further inference of this process is that the oceanic moisture is brought by the summer monsoon while the westerlies bring moisture from continental recycling or even the Mediterranean Sea, and therefore water isotope signatures reflect the interplay between the summer monsoon and westerlies (Joswiak et al., 2013; Pang et al., 2012; Tian et al., 2007). Although our results also indicate seasonally shifting moisture sources, continental recycling prevails throughout the year (Fig. 4). Besides focusing on moisture sources at the Earth surface, we provide an alternative perspective to explain the high $d$-excess induced by the westerlies as dry and cold air intrusions. In this circumstance, the interpretation of the interplay between the summer monsoon and westerlies is still valid, but we emphasize changes in air mass property driven by the different circulation systems.

The proposed alternative interpretation could also help understand the increasing trend of precipitation and river water isotope observations toward ice cores at higher altitudes on the TP as specific humidity is very low at ice core sites and prolonged interaction with cold and dry air may further modify snow isotope compositions (Ma et al., 2024; Wahl et al., 2022). In addition, intense rain-vapor interaction during the summer monsoon is another source of higher vapor $d$-excess (section 4.3). Higher vapor $d$-excess signal could be inherited in subsequent

https://doi.org/10.5194/egusphere-2024-3801
Preprint. Discussion started: 7 January 2025
© Author(s) 2025. CC BY 4.0 License.

precipitation when it feeds the precipitation (Risi et al., 2008b). However, a clear relationship between TP precipitation *d*-excess and monsoon convection has not been established yet, partly due to less attention ~~has been~~ paid to *d*-excess in previous studies. Nevertheless, summer monsoon rainfall *d*-excess observed on the TP is generally between 0-10‰ (Tian et al., 2001). Raindrop evaporation at upstream increases vapor *d*-excess and therefore could cause elevated *d*-excess in downstream rainfall. On the contrary, this effect can be compensated by on-site raindrop evaporation as it lowers raindrop *d*-excess values. The overall positive correlation between precipitation *d*-excess and altitude in Asia has been sometimes interpreted as stronger evaporation at lower altitudes (Bershaw, 2018). For snowfall on glaciers, evaporation is less likely for falling snowflakes due to cold temperatures and the short distance between the cloud base and the glacier surface. Therefore, elevated vapor *d*-excess signal caused by accumulated rain-vapor interaction at upstream associated with monsoon convection could be ~~another source for~~ the high *d*-excess in ice cores.

## 5 Conclusions

We present a three-year-long daily near-surface water vapor isotope compositions observed at the South-East TP station which is at the major channel for moisture entering the TP. Our vapor isotope compositions paired with specific humidity reflect distinct moisture sources and dynamics between the non-monsoon and summer monsoon seasons, consistent with Lagrangian moisture diagnostic results. Despite significant negative correlations between vapor *d*-excess and relative humidity scaled to sea surface temperature existing over the northern Indian Ocean when ~~data for~~ all seasons are considered, ~~such correlations with oceanic surface evaporation conditions largely disappear when separately considering each season~~. This result questions the early interpretation of TP *d*-excess as oceanic evaporation conditions and guarantees new interpretations in the future.

During the non-monsoon season, vapor *d*-excess is mainly influenced by specific humidity ~~both~~ at ~~the~~ local

https://doi.org/10.5194/egusphere-2024-3801
Preprint. Discussion started: 7 January 2025
© Author(s) 2025. CC BY 4.0 License.

scale and upstream. Highly dehydrated air at the lower end of the Rayleigh distillation is expected to have extremely high *d*-excess values. Air mass trajectory analyses and moisture source diagnostics suggest that the cold and dry air intrusion driven by the westerlies during the non-monsoon season leads to the increasing trend of vapor *d*-excess along with decreasing specific humidity. This process also contributes to a weak negative correlation between vapor *d*-excess and $\delta^{18}O$. Furthermore, vapor $\delta^{18}O$ primarily reflects mixing processes with a relatively enriched moist end-member compared with the summer monsoon season. The new insight on non-monsoon season vapor *d*-excess provides an alternative way to interpret the high *d*-excess in high-altitude TP ice cores.

During the summer monsoon season, rain evaporation is the dominant process determining water vapor isotope compositions. First, vapor $\delta^{18}O$ systematically shifts below the Rayleigh distillation curve falling in the region predicted by "super-Rayleigh" distillation driven by partial rain evaporation. Second, vapor $\delta^{18}O$ is anti-correlated with *d*-excess pointing to an origin of depleted vapor by kinetic fractionation which is not likely simply a result of rainout. Third, vapor $\delta^{18}O$ is significantly negatively correlated with total precipitation amount at the regional scale, but vapor *d*-excess positively correlates with total precipitation amount. These results help us understand the dynamics of atmospheric humidity and also help disentangle the different effects of rainout and rain-vapor interaction in the amount effect.

Overall, the new findings from the study reveal different moisture sources and dynamics between the non-monsoon and monsoon seasons over the southeastern TP. The findings will also help the interpretation of ice core $\delta^{18}O$ and *d*-excess records derived from glaciers on the TP.

**Competing interests**

The authors declare that they have no conflict of interest.

https://doi.org/10.5194/egusphere-2024-3801
Preprint. Discussion started: 7 January 2025
© Author(s) 2025. CC BY 4.0 License.

**Acknowledgements**

This research is supported by the National Natural Science Foundation of China (Grant 42371144), the Yunnan Fundamental Research Projects (Grant 202301AT070183), and the funding of Donglu Talent Young Scholar from the Yunnan University and support for young scholars from the Double First-Class Initiative for Ecological Disciplines of the Yunnan University. We would like to thank the staff at the South-East Tibetan Plateau Station for integrated observation and research of alpine environment for their help in collecting water samples and for sharing the meteorological data ~~at the station~~.

**Data availability**

The NOAA ARL provided the HYSPLIT model and the GDAS data (https://www.ready.noaa.gov/HYSPLIT.php). The Copernicus Climate Change Service provided the ERA5 data (https://doi.org/10.24381/cds.adbb2d47 and https://doi.org/10.24381/cds.f17050d7). The GPM data are available through GES DISC (https://doi.org/10.5067/GPM/IMERG/3B-HH/07). Local meteorological data at the SETP station are provided by National Tibetan Plateau / Third Pole Environment Data Center (https://dx.doi.org/10.11888/AtmosphericPhysics.tpe.68.db). The observation data at the SETP station have been uploaded to Figshare and will be made publicly available after publication (10.6084/m9.figshare.27302871).

**Author contributions**

**Zhongyin Cai**: Conceptualization, methodology, investigation, formal analysis, funding acquisition, writing-original draft, writing-review & editing; **Rong Li**: Investigation, data curation, writing-review & editing; **Cheng Wang**: Validation; **Qiukai Mao**: Investigation, **Lide Tian**: Resources, project administration, funding acquisition.

https://doi.org/10.5194/egusphere-2024-3801
Preprint. Discussion started: 7 January 2025
© Author(s) 2025. CC BY 4.0 License.

## References

Aemisegger, F., Pfahl, S., Sodemann, H., Lehner, I., Seneviratne, S. I., and Wernli, H.: Deuterium excess as a proxy for continental moisture recycling and plant transpiration, Atmos. Chem. Phys., 14, 4029-4054, 10.5194/acp-14-4029-2014, 2014.

An, W., Hou, S., Zhang, Q., Zhang, W., Wu, S., Xu, H., Pang, H., Wang, Y., and Liu, Y.: Enhanced Recent Local Moisture Recycling on the Northwestern Tibetan Plateau Deduced From Ice Core Deuterium Excess Records, J. Geophys. Res., 122, 12,541-512,556, 10.1002/2017jd027235, 2017.

Araguás-Araguás, L., Fröehlich, K., and Rozanski, K.: Stable isotope composition of precipitation over southeast Asia, J. Geophys. Res., 103, 28721-28742, 1998.

Benetti, M., Reverdin, G., Pierre, C., Merlivat, L., Risi, C., Steen-Larsen, H. C., and Vimeux, F.: Deuterium excess in marine water vapor: Dependency on relative humidity and surface wind speed during evaporation, J. Geophys. Res., 119, 584-593, 2014.

Bershaw, J.: Controls on Deuterium Excess across Asia, Geosciences, 8, 257, 10.3390/geosciences8070257, 2018.

Bonne, J.-L., Behrens, M., Meyer, H., Kipfstuhl, S., Rabe, B., Schönicke, L., Steen-Larsen, H. C., and Werner, M.: Resolving the controls of water vapour isotopes in the Atlantic sector, Nature Communications, 10, 1632, 10.1038/s41467-019-09242-6, 2019.

Bonne, J. L., Masson-Delmotte, V., Cattani, O., Delmotte, M., Risi, C., Sodemann, H., and Steen-Larsen, H. C.: The isotopic composition of water vapour and precipitation in Ivittuut, southern Greenland, Atmos. Chem. Phys., 14, 4419-4439, 10.5194/acp-14-4419-2014, 2014.

Bony, S., Risi, C., and Vimeux, F.: Influence of convective processes on the isotopic composition ($\delta^{18}O$ and $\delta D$) of precipitation and water vapor in the tropics: 1. Radiative-convective equilibrium and Tropical Ocean–Global Atmosphere–Coupled Ocean-Atmosphere Response Experiment (TOGA-COARE) simulations, J. Geophys. Res., 113, D19305, 10.1029/2008JD009942, 2008.

Bowen, G. J. and Wilkinson, B.: Spatial distribution of $\delta^{18}O$ in meteoric precipitation, Geology, 30, 315, 10.1130/0091-7613(2002)030<0315:sdooim>2.0.co;2, 2002.

Bowen, G. J., Cai, Z., Fiorella, R. P., and Putman, A.: Isotopes in the Water Cycle: Regional- to Global-Scale Patterns and Applications, Annu. Rev. Earth Planet. Sci., 47, 453-479, 10.1146/annurev-earth-053018-060220, 2019.

Breitenbach, S. F. M., Adkins, J. F., Meyer, H., Marwan, N., Kumar, K. K., and Haug, G. H.: Strong influence of water vapor source dynamics on stable isotopes in precipitation observed in Southern Meghalaya, NE India, Earth Planet. Sci. Lett., 292, 212-220, 10.1016/j.epsl.2010.01.038, 2010.

Cai, Z. and Tian, L.: Atmospheric controls on seasonal and interannual variations in the precipitation isotope in the East Asian Monsoon region, J. Climate, 29, 1339-1352, 10.1175/JCLI-D-15-0363.1, 2016.

Cai, Z. and Tian, L.: What causes the post-monsoon $^{18}O$ depletion over Bay of Bengal head and beyond?, Geophys. Res. Lett., 47, e2020GL086985, 10.1029/2020gl086985, 2020.

Cai, Z., Tian, L., and Bowen, G. J.: ENSO variability reflected in precipitation oxygen isotopes across the Asian Summer Monsoon region, Earth Planet. Sci. Lett., 475, 25-33, 10.1016/j.epsl.2017.06.035, 2017.

Cai, Z., Tian, L., and Bowen, G. J.: Spatial-seasonal patterns reveal large-scale atmospheric controls on Asian Monsoon precipitation water isotope ratios, Earth Planet. Sci. Lett., 503, 158-169, 10.1016/j.epsl.2018.09.028, 2018.

Cao, R., Huang, H., Wu, G., Han, D., Jiang, Z., Di, K., and Hu, Z.: Spatiotemporal variations in the ratio of transpiration to evapotranspiration and its controlling factors across terrestrial biomes, Agr. Forest Meteorol., 321, 108984, 10.1016/j.agrformet.2022.108984, 2022.

https://doi.org/10.5194/egusphere-2024-3801
Preprint. Discussion started: 7 January 2025
© Author(s) 2025. CC BY 4.0 License.

Chen, M., Gao, J., Luo, L., Zhao, A., Niu, X., Yu, W., Liu, Y., and Chen, G.: Temporal variations of stable isotopic compositions in atmospheric water vapor on the Southeastern Tibetan Plateau and their controlling factors, Atmos. Res., 303, 10.1016/j.atmosres.2024.107328, 2024.

Craig, H.: Isotopic Variations in Meteoric Waters, Science, 133, 1702-1703, 10.1126/science.133.3465.1702, 1961.

Craig, H. and Gordon, L. I.: Deuterium and oxygen 18 variations in the ocean and the marine atmosphere, in: Stable Isotopes in Oceanographic Studies and Paleotemperatures. Spoleto, Tongiorgi, E., Italy, 9-130, 1965.

Dai, D., Gao, J., Steen-Larsen, H. C., Yao, T., Ma, Y., Zhu, M., and Li, S.: Continuous monitoring of the isotopic composition of surface water vapor at Lhasa, southern Tibetan Plateau, Atmos. Res., 264, 10.1016/j.atmosres.2021.105827, 2021.

Dansgaard, W.: Stable isotopes in precipitation, Tellus, 16, 436-468, 10.1111/j.2153-3490.1964.tb00181.x, 1964.

Dütsch, M., Pfahl, S., and Sodemann, H.: The impact of nonequilibrium and equilibrium fractionation on two different deuterium excess definitions, J. Geophys. Res., 122, 12732-12746, 10.1002/2017JD027085, 2017.

Fiorella, R. P., Poulsen, C. J., and Matheny, A. M.: Seasonal Patterns of Water Cycling in a Deep, Continental Mountain Valley Inferred from Stable Water Vapor Isotopes, J. Geophys. Res., 123, 7271-7291, doi:10.1029/2017JD028093, 2018.

Galewsky, J., Steen-Larsen, H. C., Field, R. D., Worden, J., Risi, C., and Schneider, M.: Stable isotopes in atmospheric water vapor and applications to the hydrologic cycle, Rev. Geophys., 54, 809-865, 10.1002/2015RG000512, 2016.

Good, S. P., Noone, D., and Bowen, G.: Hydrologic connectivity constrains partitioning of global terrestrial water fluxes, Science, 349, 175-177, 10.1126/science.aaa5931, 2015.

Guo, R., Yu, W., Zhang, J., Lewis, S., Lazhu, Ma, Y., Xu, B., Wu, G., Jing, Z., Ren, P., Zhang, Z., Wang, Q., and Qu, D.: Different Dynamics Drive Indian Ocean Moisture to the Southern Slope of Central Himalayas: An Isotopic Approach, Geophys. Res. Lett., 51, 10.1029/2024gl109359, 2024.

Han, J., Tian, L., Cai, Z., Ren, W., Liu, W., Li, J., and Tai, J.: Season-specific evapotranspiration partitioning using dual water isotopes in a Pinus yunnanensis ecosystem, southwest China, J. Hydrol., 608, 127672, 10.1016/j.jhydrol.2022.127672, 2022.

He, Y., Risi, C., Gao, J., Masson-Delmotte, V., Yao, T., Lai, C.-T., Ding, Y., Worden, J., Frankenberg, C., Chepfer, H., and Cesana, G.: Impact of atmospheric convection on south Tibet summer precipitation isotopologue composition using a combination of in situ measurements, satellite data and atmospheric general circulation modeling, J. Geophys. Res., 120, 3852-3871, 10.1002/2014JD022180, 2015.

Hersbach, H., Bell, W., Berrisford, P., Horányi, A., J., M.-S., Nicolas, J., Radu, R., Schepers, D., Simmons, A., Soci, C., and Dee, D.: Global reanalysis: goodbye ERA-Interim, hello ERA5, 10.21957/vf291hehd7, 2019.

Huffman, G. J., Stocker, E. F., Bolvin, D. T., Nelkin, E. J., and Tan, J.: GPM IMERG Final Precipitation L3 Half Hourly 0.1 degree x 0.1 degree V07, Greenbelt, MD, Goddard Earth Sciences Data and Information Services Center (GES DISC) [dataset], 10.5067/GPM/IMERG/3B-HH/07, 2023.

Jiang, J., Zhou, T., Qian, Y., Li, C., Song, F., Li, H., Chen, X., Zhang, W., and Chen, Z.: Precipitation regime changes in High Mountain Asia driven by cleaner air, Nature, 10.1038/s41586-023-06619-y, 2023.

Joswiak, D. R., Yao, T., Wu, G., Tian, L., and Xu, B.: Ice-core evidence of westerly and monsoon moisture contributions in the central Tibetan Plateau, J. Glaciol., 59, 56-66, 10.3189/2013JoG12J035, 2013.

Keeling, C. D.: The concentration and isotopic abundances of atmospheric carbon dioxide in rural areas, Geochim. Cosmochim. Acta, 13, 322-334, 10.1016/0016-7037(58)90033-4, 1958.

Kurita, N., Noone, D., Risi, C., Schmidt, G. A., Yamada, H., and Yoneyama, K.: Intraseasonal isotopic variation associated with the Madden-Julian Oscillation, J. Geophys. Res., 116, D24101, 10.1029/2010JD015209, 2011.

Lawrence, J. R., Gedzelman, S. D., Dexheimer, D., Cho, H.-K., Carrie, G. D., Gasparini, R., Anderson, C. R.,

https://doi.org/10.5194/egusphere-2024-3801
Preprint. Discussion started: 7 January 2025
© Author(s) 2025. CC BY 4.0 License.

Bowman, K. P., and Biggerstaff, M. I.: Stable isotopic composition of water vapor in the tropics, J. Geophys. Res., 109, D06115, 10.1029/2003JD004046, 2004.

Lee, J.-E. and Fung, I.: "Amount effect" of water isotopes and quantitative analysis of post-condensation processes, Hydrol. Processes, 22, 1-8, 10.1002/hyp.6637, 2008.

Lekshmy, P. R., Midhun, M., and Ramesh, R.: Role of moisture transport from Western Pacific region on water vapor isotopes over the Bay of Bengal, Atmos. Res., 265, 10.1016/j.atmosres.2021.105895, 2022.

Liu, F., Tian, L., Cai, Z., Wang, X., Liang, P., Wang, S., and Li, S.: What caused the lag between oxygen-18 and deuterium excess in atmospheric vapor and precipitation during the earlier summer season in southwest China?, J. Hydrol., 644, 10.1016/j.jhydrol.2024.132087, 2024.

Liu, J., Xiao, C., Ding, M., and Ren, J.: Variations in stable hydrogen and oxygen isotopes in atmospheric water vapor in the marine boundary layer across a wide latitude range, Journal of Environmental Sciences, 26, 2266-2276, 10.1016/j.jes.2014.09.007, 2014.

Luo, L.: Meteorological observation data from the integrated observation and research station of the alpine environment in Southeast Tibet (2007-2017), National Tibetan Plateau Data Center [dataset], 10.11888/AtmosphericPhysics.tpe.68.db, 2018.

Ma, T., Jiang, Z., Ding, M., He, P., Li, Y., Zhang, W., and Geng, L.: A model framework for atmosphere–snow water vapor exchange and the associated isotope effects at Dome Argus, Antarctica – Part 1: The diurnal changes, The Cryosphere, 18, 4547-4565, 10.5194/tc-18-4547-2024, 2024.

Merlivat, L. and Jouzel, J.: Global climatic interpretation of the deuterium-oxygen 18 relationship for precipitation, J. Geophys. Res., 84, 5029-5033, 1979.

Noone, D.: Pairing Measurements of the Water Vapor Isotope Ratio with Humidity to Deduce Atmospheric Moistening and Dehydration in the Tropical Midtroposphere, J. Climate, 25, 4476-4494, 10.1175/jcli-d-11-00582.1, 2012.

Pang, H., Hou, S., Kaspari, S., Mayewski, P., Introne, D., Masson-Delmotte, V., Jouzel, J., Li, Z., He, Y., Hong, S., and Qin, D.: Atmospheric circulation change in the central Himalayas indicated by a high-resolution ice core deuterium excess record, Climate Research, 53, 1-12, 10.3354/cr01090, 2012.

Putman, A. L., Fiorella, R. P., Bowen, G. J., and Cai, Z.: A Global Perspective on Local Meteoric Water Lines: Meta-analytic Insight into Fundamental Controls and Practical Constraints, Water Resour. Res., 55, 6896-6910, 10.1029/2019wr025181, 2019.

Risi, C., Bony, S., and Vimeux, F.: Influence of convective processes on the isotopic composition ($\delta^{18}O$ and $\delta D$) of precipitation and water vapor in the tropics: 2. Physical interpretation of the amount effect, J. Geophys. Res., 113, D19306, 10.1029/2008JD009943, 2008a.

Risi, C., Bony, S., Vimeux, F., Descroix, L., Ibrahim, B., Lebreton, E., Mamadou, I., and Sultan, B.: What controls the isotopic composition of the African monsoon precipitation? Insights from event-based precipitation collected during the 2006 AMMA field campaign, Geophys. Res. Lett., 35, L24808, 10.1029/2008GL035920, 2008b.

Samuels-Crow, K. E., Galewsky, J., Sharp, Z. D., and Dennis, K. J.: Deuterium excess in subtropical free troposphere water vapor: Continuous measurements from the Chajnantor Plateau, northern Chile, Geophys. Res. Lett., 41, 8652-8659, 10.1002/2014gl062302, 2014.

Sayres, D. S., Pfister, L., Hanisco, T. F., Moyer, E. J., Smith, J. B., St. Clair, J. M., O'Brien, A. S., Witinski, M. F., Legg, M., and Anderson, J. G.: Influence of convection on the water isotopic composition of the tropical tropopause layer and tropical stratosphere, J. Geophys. Res., 115, 10.1029/2009JD013100, 2010.

Scholl, M. A., Shanley, J. B., Zegarra, J. P., and Coplen, T. B.: The stable isotope amount effect: New insights from NEXRAD echo tops, Luquillo Mountains, Puerto Rico, Water Resour. Res., 45, 10.1029/2008wr007515, 2009.

Shao, L., Tian, L., Cai, Z., Wang, C., and Li, Y.: Large-scale atmospheric circulation influences the ice core d-excess record from the central Tibetan Plateau, Clim. Dyn., 57, 1805-1816, 10.1007/s00382-021-05779-9, 2021.

Sodemann, H., Schwierz, C., and Wernli, H.: Interannual variability of Greenland winter precipitation sources: Lagrangian moisture diagnostic and North Atlantic Oscillation influence, J. Geophys. Res., 113, 10.1029/2007jd008503, 2008.

Sodemann, H., Aemisegger, F., Pfahl, S., Bitter, M., Corsmeier, U., Feuerle, T., Graf, P., Hankers, R., Hsiao, G., Schulz, H., Wieser, A., and Wernli, H.: The stable isotopic composition of water vapour above Corsica during the HyMeX SOP1 campaign: insight into vertical mixing processes from lower-tropospheric survey flights, Atmos. Chem. Phys., 17, 6125-6151, 10.5194/acp-17-6125-2017, 2017.

Steen-Larsen, H. C., Risi, C., Werner, M., Yoshimura, K., and Masson-Delmotte, V.: Evaluating the skills of isotope-enabled General Circulation Models against in-situ atmospheric water vapor isotope observations, J. Geophys. Res., 122, 246-263, 10.1002/2016JD025443, 2017.

Stein, A. F., Draxler, R. R., Rolph, G. D., Stunder, B. J. B., Cohen, M. D., and Ngan, F.: NOAA's HYSPLIT atmospheric transport and dispersion modeling system, Bull. Am. Meteorol. Soc., 96, 2059-2077, 10.1175/BAMS-D-14-00110.1, 2015.

Terzer-Wassmuth, S., Wassenaar, L. I., Welker, J. M., and Araguas-Araguas, L. J.: Improved High-Resolution Global and Regionalized Isoscapes of δ18O, δ2H, and d-Excess in Precipitation, Hydrol. Processes, 35, 10.1002/hyp.14254, 2021.

Thompson, L. G., Yao, T., E.Mosley-Thompson, Davis, M. E., Henderson, K. A., and Lin, P.-N.: A High-Resolution Millennial Record of the South Asian Monsoon from Himalayan Ice Cores, Science, 289, 1916-1919, 10.1126/science.289.5486.1916, 2000.

Thompson, L. G., Yao, T. D., Davis, M. E., Mosley-Thompson, E., Synal, H. A., Wu, G., Bolzan, J. F., Kutuzov, S., Beaudon, E., Sierra-Hernández, M. R., and Beer, J.: Ice core evidence for an orbital-scale climate transition on the Northwest Tibetan Plateau, Quat. Sci. Rev., 324, 10.1016/j.quascirev.2023.108443, 2024.

Tian, L., Masson-Delmotte, V., Stievenard, M., Yao, T., and Jouzel, J.: Tibetan Plateau summer monsoon northward extent revealed by measurements of water stable isotopes, J. Geophys. Res., 106, 28081-28088, 10.1029/2001JD900186, 2001.

Tian, L., Yao, T., MacClune, K., White, J. W. C., Schilla, A., Vaughn, B., Vachon, R., and Ichiyanagi, K.: Stable isotopic variations in west China: A consideration of moisture sources, J. Geophys. Res., 112, D10112, 10.1029/2006jd007718, 2007.

Tian, L., Yu, W., Schuster, P. F., Wen, R., Cai, Z., Wang, D., Shao, L., Cui, J., and Guo, X.: Control of seasonal water vapor isotope variations at Lhasa, southern Tibetan Plateau, J. Hydrol., 580, 124237, 10.1016/j.jhydrol.2019.124237, 2020.

Uemura, R., Matsui, Y., Yoshimura, K., Motoyama, H., and Yoshida, N.: Evidence of deuterium excess in water vapor as an indicator of ocean surface conditions, J. Geophys. Res., 113, 10.1029/2008jd010209, 2008.

Vuille, M., Bradley, R. S., Werner, M., Healy, R., and Keimig, F.: Modeling $\delta^{18}O$ in precipitation over the tropical Americas: 1. Interannual variability and climatic controls, J. Geophys. Res., 108, 4174, 10.1029/2001JD002038, 2003.

Wahl, S., Steen-Larsen, H. C., Hughes, A. G., Dietrich, L. J., Zuhr, A., Behrens, M., Faber, A.-K., and Hörhold, M.: Atmosphere-Snow Exchange Explains Surface Snow Isotope Variability, Geophys. Res. Lett., 49, e2022GL099529, 10.1029/2022GL099529, 2022.

Webster, C. R. and Heymsfield, A. J.: Water isotope ratios D/H, 18O/16O, 17O/16O in and out of clouds map dehydration pathways, Science, 302, 1742-1745, 10.1126/science.1089496, 2003.

Wei, Z. and Lee, X.: The utility of near-surface water vapor deuterium excess as an indicator of atmospheric moisture source, J. Hydrol., 123923, 10.1016/j.jhydrol.2019.123923, 2019.

Welp, L. R., Lee, X., Griffis, T. J., Wen, X. F., Xiao, W., Li, S., Sun, X., Hu, Z., Val Martin, M., and Huang, J.: A meta-analysis of water vapor deuterium-excess in the midlatitude atmospheric surface layer, Global Biogeochem. Cycles, 26, 10.1029/2011gb004246, 2012.

https://doi.org/10.5194/egusphere-2024-3801
Preprint. Discussion started: 7 January 2025
© Author(s) 2025. CC BY 4.0 License.

Worden, J., Noone, D., and Bowman, K.: Importance of rain evaporation and continental convection in the tropical water cycle, Nature, 445, 528-532, 10.1038/nature05508, 2007.

Wu, F., Fang, X., Yang, Y., Dupont-Nivet, G., Nie, J., Fluteau, F., Zhang, T., and Han, W.: Reorganization of Asian climate in relation to Tibetan Plateau uplift, Nature Reviews Earth & Environment, 10.1038/s43017-022-00331-7, 2022.

Yang, X. and Yao, T.: Seasonality of moisture supplies to precipitation over the Third Pole: a stable water isotopic perspective, Sci Rep, 10, 15020, 10.1038/s41598-020-71949-0, 2020.

Yang, X., Davis, M. E., Acharya, S., and Yao, T.: Asian monsoon variations revealed from stable isotopes in precipitation, Clim. Dyn., 51, 2267-2283, 10.1007/s00382-017-4011-4, 2017.

Yao, T., Masson-Delmotte, V., Gao, J., Yu, W., Yang, X., Risi, C., Sturm, C., Werner, M., Zhao, H., He, Y., Ren, W., Tian, L., Shi, C., and Hou, S.: A review of climatic controls on $\delta^{18}O$ in precipitation over the Tibetan Plateau: Observations and simulations, Rev. Geophys., 51, 525-548, 10.1002/rog.20023, 2013.

Yao, T., Bolch, T., Chen, D., Gao, J., Immerzeel, W., Piao, S., Su, F., Thompson, L., Wada, Y., Wang, L., Wang, T., Wu, G., Xu, B., Yang, W., Zhang, G., and Zhao, P.: The imbalance of the Asian water tower, Nature Reviews Earth & Environment, 3, 618-632, 10.1038/s43017-022-00299-4, 2022.

Yu, W., Tian, L., Ma, Y., Xu, B., and Qu, D.: Simultaneous monitoring of stable oxygen isotope composition in water vapour and precipitation over the central Tibetan Plateau, Atmos. Chem. Phys., 15, 10251-10262, 10.5194/acp-15-10251-2015, 2015.

Yu, W., Tian, L., Risi, C., Yao, T., Ma, Y., Zhao, H., Zhu, H., He, Y., Xu, B., Zhang, H., and Qu, D.: $\delta^{18}O$ records in water vapor and an ice core from the eastern Pamir Plateau: Implications for paleoclimate reconstructions, Earth Planet. Sci. Lett., 456, 146-156, 10.1016/j.epsl.2016.10.001, 2016.

Zhang, Q., Shen, Z., Pokhrel, Y., Farinotti, D., Singh, V. P., Xu, C.-Y., Wu, W., and Wang, G.: Oceanic climate changes threaten the sustainability of Asia's water tower, Nature, 615, 87-93, 10.1038/s41586-022-05643-8, 2023.

Zhao, H., Xu, B., Li, Z., Wang, M., Li, J., and Zhang, X.: Abundant climatic information in water stable isotope record from a maritime glacier on southeastern Tibetan Plateau, Clim. Dyn., 48, 1161-1171, 10.1007/s00382-016-3133-4, 2017.

Zhao, H., Xu, B., Yao, T., Wu, G., Lin, S., Gao, J., and Wang, M.: Deuterium excess record in a southern Tibetan ice core and its potential climatic implications, Clim. Dyn., 38, 1791-1803, 10.1007/s00382-011-1161-7, 2012.